

^{57}Fe Mössbauer study of chromium-doped magnetite, $\text{Fe}_{3-x}\text{Cr}_x\text{O}_4$ ($0 \leq x \leq 0.5$) above the Verwey transition

Hang Nam Ok,* Lu San Pan, and B. J. Evans

Department of Chemistry, The University of Michigan, Ann Arbor, Michigan 48109

(Received 23 June 1976; revised manuscript received 7 February 1977)

^{57}Fe Mössbauer measurements show that the ratio of the integrated intensities of the ^{57}Fe *A*- and *B*-site Mössbauer subspectra is in good agreement with those expected for the cation distribution $(\text{Fe}^{3+})_x(\text{Fe}^{2+}\text{Cr}_x)\text{O}_4$, $0 \leq x \leq 0.3$. The magnetic moments are also found to be in good agreement with this cation distribution. The compositional dependences of the Mössbauer hyperfine parameters display no features in this compositional range that would result from a qualitative change in electronic structure. The observed line broadening and line shapes are readily accounted for by the local configurations of ions resulting from a random substitution of Cr^{3+} on the *B* sites. Consequently, the conduction mechanism in these doped magnetites is similar to that in pure Fe_3O_4 . The marked changes in the spectra for $x \approx 0.5$ are due primarily to the commencement of the occupation of the *A* site by Fe^{2+} ions and the change of the Mössbauer parameters between $x = 0.3$ and $x = 0.5$ are as expected if *A*-site Fe^{2+} ions are present.

I. INTRODUCTION

Extensive studies of the spinel system $\text{Fe}_{3-x}\text{Cr}_x\text{O}_4$ ($0 \leq x \leq 2$) have been carried out by Robbins *et al.*¹ using x-ray, magnetic, and Mössbauer techniques. Our attention was especially attracted by their results on the site distributions and conduction mechanism in the samples with low chromium contents. It was suggested mainly on the basis of the absorption area ratios of the two Mössbauer subspectra that the electron delocalization mechanism for iron ions at the *B* (octahedral) sites is by means of pairwise hopping among Fe^{2+} - Fe^{3+} pairs for $x \leq 0.5$. However, a more recent Mössbauer measurement² showed a very low value for the absorption area ratio in the case of $x = 0.25$ raising doubts about the results in the earlier study.¹

Because of the current interests in the low-temperature phase transition, the Verwey transition, in Fe_3O_4 and the necessity of an understanding of the conduction mechanism in the high-temperature phase to the assessment of the roles of electronic and structural factors in the complex Verwey transition, we have reinvestigated the system $\text{Fe}_{3-x}\text{Cr}_x\text{O}_4$. The investigation reported on here has had two major objectives: First, through careful measurements at small increments of x in $\text{Fe}_{3-x}\text{Cr}_x\text{O}_4$, $x \leq 0.5$, a resolution of the controversy on the area ratios resulting from previous studies^{1,2} has been sought. Second, the ^{57}Fe Mössbauer data have been evaluated rigorously in comparison to the predictions of a localized hopping model (primarily the pairwise hopping model) and a band model in hopes of either establishing the validity of one of these models or the inadequacy of the Mössbauer spectra as a test of either.

In magnetite,³ the iron ions are located either at *A* (tetrahedral) or *B* (octahedral) sites, and the

major exchange interaction responsible for the magnetic ordering is the strong antiferromagnetic *A*-*B* interaction. Since the *A*-*A* and *B*-*B* interactions are weak, magnetite has ferromagnetic ordering in which all the spins on a given sublattice are parallel to each other but are antiparallel to the spins on the other sublattice. Thus, the substitution of Cr^{3+} ions for *B*-site iron ions leads to a replacement of antiferromagnetic $\text{Fe}(A)\text{-O-Fe}(B)$ linkages by the $\text{Fe}(A)\text{-O-Cr}(B)$ linkages which are also likely to be antiferromagnetic since antiferromagnetic exchange interactions are observed⁴ for $\text{Fe}^{3+}\text{-O-Cr}^{3+}$ linkages when the Fe-O-Cr angle is 150° and the *A*-*O*-*B* bond angle of 126° is sufficiently close to this value that no marked change in exchange interactions is expected. Magnetic-moment measurements¹ also support the antiferromagnetic nature of the $\text{Fe}(A)\text{-O-Cr}(B)$ exchange interaction. On the other hand, the chromium substitution replaces the $90^\circ \text{Fe}(B)\text{-O-Fe}(B)$ configuration by the $90^\circ \text{Fe}(B)\text{-O-Cr}(B)$ configuration. While both direct and superexchange interactions are very small for $90^\circ \text{Fe}^{3+}\text{-O-Fe}^{3+}$, direct-exchange interactions between the two magnetic ions in the $90^\circ \text{Fe}(B)\text{-O-Cr}(B)$ configuration are expected to be significant because of the large $90^\circ \text{Cr}^{3+}\text{-O-Cr}^{3+}$ direct-exchange interactions.⁵ In the case of LiCrO_3 , the $\text{Cr}^{3+}\text{-O-Cr}^{3+}$ angle is 92.8° and the asymptotic Curie temperature⁵ Θ is -577 K. In magnetite the *B*-*O*-*B* angle⁶ is 91.9° and since the direct-exchange interaction rapidly increases with decreasing bond angle,⁵ the direct $\text{Fe}(B)\text{-O-Cr}(B)$ exchange may have a Θ value with a magnitude in excess of 600°K . Therefore, the increasing broadening^{1,2} of the Mössbauer lines of the *B* patterns with increasing substitution of Cr ions in magnetite may be due mainly to the distributions⁷ of Cr ions among the six nearest-neighbor *B* sites around

a *B*-site Fe ion.

In this work we have prepared low-concentration Cr-substituted magnetites with $x \leq 0.5$ and analyzed their Mössbauer spectra on the basis of the probability of the distribution of different numbers of Cr ions about a given *B* site to obtain information on the site distributions and conduction mechanism in these materials. These probability distributions have been analyzed under the assumption of random, intrasite occupation. In addition to the objectives mentioned above, the effects of conduction-electron concentration on the magnetic hyperfine field and isomer shift at the *B* site have also been examined.

II. EXPERIMENTAL

The $\text{Fe}_{3-x}\text{Cr}_x\text{O}_4$ ($x = 0, 0.05, \frac{1}{8}, \frac{1}{4}, \frac{3}{8}, \frac{1}{2}$) samples were prepared by grinding together appropriate proportions of high-purity (Johnson-Matthey specpure grade) ferric oxide, chromium oxide, and iron powder, pressing the resulting mixture into pellets at a pressure of 6000 kg/cm^2 and firing in evacuated quartz tubes at 1000°C for 48 h. The grinding, pressing, and firing operations were repeated at least once. X-ray powder photographs of the samples were taken with a focussed Guinier camera, using $\text{CuK}\alpha_1$ radiation and the diffraction patterns showed only the presence of a single spinel phase. Intimate mixtures of Fe_3O_4 and Cr_2O_3 , containing between 5 and 1% by weight Cr_2O_3 , were prepared and their x-ray powder patterns obtained. It is possible with our instrumentation to detect 1% Cr_2O_3 in Fe_3O_4 and since no evidence for Cr_2O_3 was observed in the powder patterns of $\text{Fe}_{3-x}\text{Cr}_x\text{O}_4$, any unreacted Cr_2O_3 must present at less than 1 wt. %. For x values exceeding 0.5, the refractory nature of Cr_2O_3 is expected to lead to some unreacted Cr_2O_3 in the final products prepared by the above technique; and indeed, we could not prepare FeCr_2O_4 by this technique. No difficulties arising from unreacted starting materials are manifest in either the x-ray or Mössbauer results. The lattice constants obtained from powder patterns having a silicon internal standard are tabulated in Table I and are in good agreement with the most

TABLE I. Lattice constants of $\text{Fe}_{3-x}\text{Cr}_x\text{O}_4$ at 298 K.

x	a_0 (10^{-8} cm)
0	8.396 ₃
0.05	8.395 ₃
0.125	8.392 ₃
0.25	8.388 ₃
0.375	8.384 ₃
0.5	8.382 ₃

recently published values.¹ It may be noticed that the lattice parameters decreased with increasing chromium doping level in conformity with the smaller ionic radius of Cr^{3+} compared to the Fe^{3+} .

The Mössbauer absorbers were prepared in the form of plastic disks of about 0.5 mm thickness by mixing the samples with a thermosetting transparent Lucite powder and heating to 423 K under pressure in a 1-in. die. The absorber thickness was approximately 10 mg/cm^2 of natural iron. The Mössbauer spectra were obtained at room temperature with an electromechanical transducer operating in a constant-acceleration mode in conjunction with 1024-channel analyzer. A 40-mCi ^{57}Co source in rhodium metal was used for all measurements.

The spectra were analyzed by means of a least-mean-squares fitting technique. The lines of the calculated spectrum were assumed to be Lorentzian in shape.

III. RESULTS

Mössbauer spectra of $\text{Fe}_{3-x}\text{Cr}_x\text{O}_4$ ($x = 0, 0.05, 0.125, 0.25, 0.375, \text{ and } 0.5$) were obtained at 300 K and some of them are shown in Fig. 1. Assigning the sharper six-line pattern (hereafter termed the *A* subspectrum) to a well-defined +3 oxidation state of Fe, the broader pattern (hereafter termed the *B* subspectrum) would then originate from a less well-defined oxidation state of Fe. As mentioned in the Introduction, the broadening of the *B* pattern may be interpreted as being due to a distribution of hyperfine fields at the *B*-site Fe ions caused by variations in the number of Cr^{3+} ions among the six nearest-neighbor *B* sites. The hyperfine fields for the locally different *B* sites are assumed to obey the following relationship⁷:

$$H_n = H_0 - n\Delta H, \quad (1)$$

where n is the number of Cr neighbors among the six nearest-neighbor *B* sites of the *B*-site Fe ion that has a hyperfine field H_n . H_0 is the hyperfine field at a *B*-site Fe ion that has no Cr *B*-site neighbors. The relative intensity of the different *B*-site spectra is given by

$$P(n, x) = \binom{6}{n} \left(\frac{1}{2}x\right)^n (1 - \frac{1}{2}x)^{6-n}, \quad (2)$$

where $\frac{1}{2}x$ is the number of Cr ions per *B* site. The calculated values of $P(n, x)$ relevant to this work are shown in Table II. This relationship is based on the assumption of a random occupation of the *B* sites by Cr^{3+} . There is no direct evidence for this assumption but more sophisticated *a priori* assumptions require a precision in the data not ob-

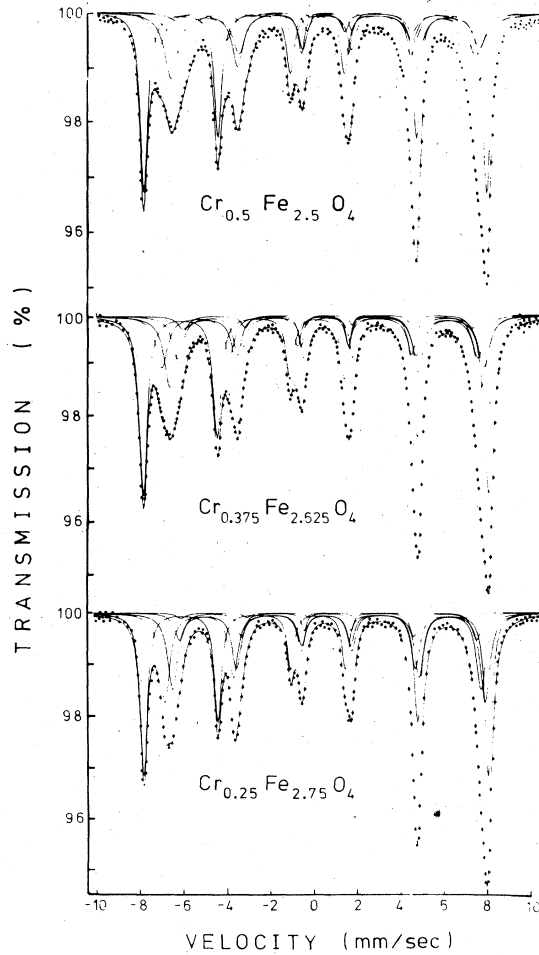


FIG. 1. ^{57}Fe ME spectra of $\text{Cr}_x\text{Fe}_{3-x}\text{O}_4$. The solid lines through the data points are the results of a least-squares fit of several sets of six-line (Lorentzian) patterns to the experimental data. The solid lines above the data points are the individual component lines.

tainable for the large linewidths and small hyperfine field variations encountered in this system. In addition, the effects of nonrandom occupation of the B site by Cr have been minimized by the low Cr contents employed. There may also be higher-

TABLE II. Probability $P(n, x)$ of a B site having n Cr ions at the nearest B sites for $\text{Fe}_{3-x}\text{Cr}_x\text{O}_4$.

n	Value of x			
	0.125	0.25	0.375	0.5
0	0.679	0.449	0.288	0.178
1	0.272	0.385	0.398	0.356
2	0.045	0.137	0.230	0.297
3	0.004	0.026	0.071	0.132
4	0.000	0.003	0.012	0.033
5	0.000	0.000	0.001	0.004

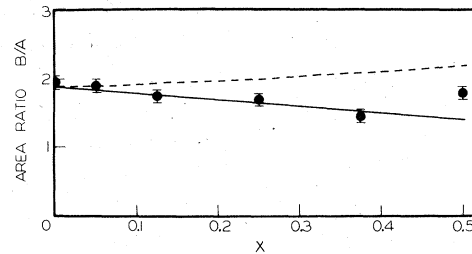


FIG. 2. Area ratio of the B to A subspectra.

order terms on the right-hand side of Eq. (1) but again the large linewidths and small variations in hyperfine fields make the fitting of the spectra to such a relationship of very doubtful value.

Only one six-line pattern was needed to obtain an acceptable fit to the A subspectrum for all values of $x < 0.5$; n such patterns were fitted to the B subspectrum subject to the constraint that

$$\sum_{i=0}^n P(i, x) \geq 0.99, \quad (3)$$

in addition to those in Eqs. (1) and (2). The widths and overall intensities of the A and B subspectra were independently varied as free parameters. However, within a subspectrum the following constraints were imposed:

$$\Gamma_i = \Gamma_{7-i} \quad \text{and} \quad I_i = I_{7-i}, \quad (4)$$

where Γ_i and I_i represent the linewidths and intensities, respectively; and i goes from 1 to 3. The quadrupole splitting ΔE_q and the isomer shift δ were independently varied for each of the subspectra.

The results of the least-mean-squares fitting are shown in Figs. 2 and 3 and in Tables III and IV. The solid lines through the data points in Fig. 1 are the envelopes of all the subspectra. The linewidths in Table IV are quite similar to those observed for insulating, inverse spinel ferrites.⁸

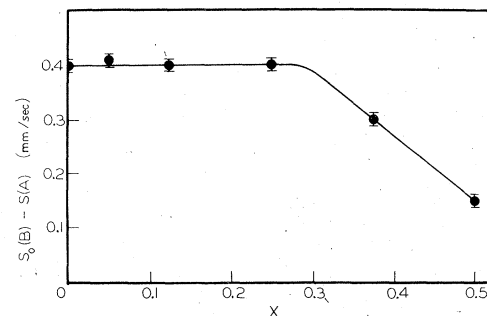


FIG. 3. Isomer shift difference between B -site iron ions with $n=0$ and A -site ferric ions.

IV. DISCUSSION

A. Area ratios of *A* and *B* subspectra

As shown in Table III and Fig. 2, the area ratios of the *A* and *B* subspectra as fitted in this study are in good quantitative agreement with that expected if all the Fe ions on the *A* site are ferric and if all the *B*-site Fe ions contribute to the *B* subspectra. The area ratio of the *B* to *A* subspectra is equal to the following expression when all of the *B*-site Fe ions contribute to the *B* subspectra and all the *A*-site ions are ferric:

$$A_\beta/A_\alpha = [(2-x)/1] f_\beta/f_\alpha, \quad (5a)$$

where f_β/f_α is the ratio of the recoil-free fractions of *B*- and *A*-site Fe ions at 298 K. Using the value of 0.94 for f_β/f_α ,⁹ Eq. (4) was solved for each *x* value and the results are shown in the column 3 of Table III and plotted as the solid line in Fig. 2. It should be noted that our experimental values of A_β/A_α exhibit a significant decrease with increasing *x* values until *x* approaches 0.5 at which point A_β/A_α shows an increasing trend. This decrease in A_β/A_α with *x* is in contrast to the constant value of about 2 for $0 \leq x \leq 0.5$ reported previously.¹

In order to understand the origin of these discrepancies, 2 sets of 6 lines (one each for the *A* and *B* subspectra) were fitted to the Mössbauer spectra even though the fits did not meet the goodness-of-fit criterion due to the non-Lorentzian line shape of the *B* subspectra. From these fits A_β/A_α values in better agreement with those reported earlier were obtained¹; for example, from these fits A_β/A_α is 1.92 for *x* = 0.25. Clearly, such fits, however, are inadequate as quantitative fits to the spectra. Even though the quantitative aspects of the spectra were not a major concern in one of the earlier studies,¹ it is clear that the neglect of these quantitative aspects leads to inaccurate area ratios. Because the A_β/A_α area ratio is a sensitive parameter in models of the conduction mecha-

TABLE III. Area ratio of the *A* and *B* subspectra.

<i>x</i>	A_β/A_α ^a	A'_β/A'_α ^b	A''_β/A''_α ^c
0	1.96 ₈ ^d	1.88 ^e	1.88 ^e
0.05	1.89 ₈	1.83	1.90
0.125	1.75 ₉	1.76	1.94
0.25	1.70 ₉	1.64	2.01
0.375	1.44 ₉	1.53	2.10
0.5	1.80 ₉	1.41	2.19

^a Experimental value.

^b Calculated according to Eq. (5a).

^c Calculated according to Eq. (5d).

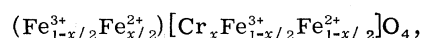
^d Subscript below each number indicates estimated error in the last digit.

^e A value of 0.94 for f_β/f_α was used in calculating A'_β/A'_α and A''_β/A''_α .

nisms, adequate spectral fits are necessary if conclusions are to be drawn concerning the conduction mechanism, as will be seen below.

The values of A_β/A_α resulting from this investigation would require a band model for the conduction mechanism in Fe_3O_4 , as well as for $\text{Fe}_{3-x}\text{Cr}_x\text{O}_4$ for *x* < 0.5. On the other hand, it was concluded previously¹ that a localized, pairwise hopping was consistent with the values of A_β/A_α , and even though it is clear that the values of A_β/A_α were incorrect as deduced in the earlier measurements, it is instructive to reconsider these data so as to provide a definitive resolution of the discrepancies.

For *x* < 0.5, the following cation distribution was proposed¹:



where the ions in the parentheses are located at *A* sites and those in brackets at *B* sites. The ferrous ions at *A* sites have been assumed by us to contribute to *B* subspectra because the sharp *A* subspectrum does not seem to be composite and it has ⁵⁷Fe Mössbauer hyperfine parameters in close correspondence to those of Fe³⁺ ions in insulating ferrites.⁹ It was observed earlier¹ that the *A* subspec-

TABLE IV. Selected results of least-squares fits of 2–6 sets of six-line patterns to the Mössbauer spectra of $\text{Fe}_{3-x}\text{Cr}_x\text{O}_4$ at 298 K.

<i>x</i>	H_A (kOe)	H_0 (kOe)	ΔH (kOe)	$S_0 - S_A$ (mm/sec)	H_0/H_A	$(\Delta E_Q)_A$ (mm/sec)	$(\Delta E_Q)_0$ (mm/sec)	Γ_A (FWHM) ^a (mm/sec)	Γ_B (FWHM) (mm/sec)
0	496 ₂ ^b	460 ₂		0.40 ₁	0.927 ₈	-0.04 ₁	0.00 ₂	0.340 ₂	0.400 ₂
0.5	495 ₂	458 ₂		0.41 ₁	0.925 ₈	-0.04 ₁	0.00 ₂	0.33 ₁	0.40 ₁
0.125	494 ₂	457 ₂	11 ₂	0.40 ₁	0.925 ₈	-0.04 ₁	-0.03 ₂	0.34 ₁	0.48 ₁
0.25	491 ₂	456 ₃	17 ₃	0.40 ₁	0.929 ₉	-0.04 ₁	-0.03 ₂	0.37 ₁	0.43 ₁
0.375	490 ₂	457 ₃	16 ₃	0.30 ₁	0.933 ₉	-0.04 ₁	0.00 ₂	0.42 ₁	0.46 ₂
0.5	487 ₂	456 ₃	17 ₃	0.15 ₁	0.936 ₉	-0.04 ₁	0.00 ₂	0.41 ₁	0.50 ₂

^a FWHM: full width at half maximum.

^b Subscript below each number indicates estimated error in the last digit.

trum had narrow lines and Mössbauer parameters corresponding to a well-defined Fe^{3+} species. It was assumed, however, that the A -site Fe^{2+} contributed to neither the A nor B subspectrum. We could find no evidence of an Fe^{2+} pattern for $x < 0.5$ which contributed to neither the A nor B subspectrum and since the Mössbauer parameters of an A -site Fe^{2+} ion would be closer to those of the B subspectrum, we have included the contribution of $(\text{Fe}^{2+})_{A \text{ site}}$ to the integrated intensity of the B subspectrum, A_β in our formulation of Eq. (5a). The effect of this term is small, however, for $x \leq 0.5$ and regardless of whether the A -site Fe^{2+} contribution to the spectrum is neglected or not, the data from this investigation permit the validity of the localized hopping model to be tested. According to this model, the absorption area ratio would be equal to the following expression:

$$\frac{A_\beta}{A_\alpha} = \frac{2(\text{Fe}^{2+} \rightleftharpoons \text{Fe}^{3+})_{B \text{ site pairs}} + (\text{Fe}^{2+})_{A \text{ site}}}{[\text{Fe}^{3+}]_{A \text{ site}}} \frac{f_\beta}{f_\alpha}, \quad (5b)$$

$$\frac{A_\beta}{A_\alpha} = \frac{2(1 - \frac{1}{2}x) + \frac{1}{2}x}{1 - \frac{1}{2}x} \frac{f_\beta}{f_\alpha}, \quad (5c)$$

$$A_\beta/A_\alpha = [(4-x)/(2-x)](f_\beta/f_\alpha). \quad (5d)$$

The calculated values of Eq. (5a) using $f_\beta/f_\alpha = 0.94$ are shown in the fourth column of Table III and are plotted as the broken line in Fig. 2. The values are nearly 2 and increase slowly as x increases, which is in disagreement with our data in Fig. 2 unless x is close to 0.5. Our data show that as x increases beyond 0.3, some Fe^{2+} start to go over to the A sites but the number of Fe^{2+} ions on A sites is substantially smaller than that required for a B -site distribution optimized for pairwise hopping; for example, for the $x = 0.5$ case, our area ratio value of 1.80 gives 0.14 for the fraction of Fe^{2+} ions at A sites which is about half the value of 0.25 required for an optimal pairwise $\text{Fe}^{3+} \rightarrow \text{Fe}^{2+}$ B -site occupation.

Thus, the area ratio A_β/A_α is in disagreement with the predictions of a localized, hopping model for the electronic conduction mechanism in pure and lightly doped Fe_3O_4 above the Verwey transition but is in good agreement with the predictions of band conduction. The advantage of studying substituted (doped) Fe_3O_4 at low substitution levels and for substituents with well-defined local crystal chemistries is clearly evident, as it is not possible to distinguish between band conduction and localized, pairwise hopping in pure Fe_3O_4 . Further, indirect support of band conduction is provided by the absence of any evidence for incipient Fe^{2+} B -site ions for $x < 0.3$. If the strength of the electron delocalization had been so weak as to result only in

electron hopping in pure Fe_3O_4 , then the presence of impurity levels approaching 13% of the B sites should have resulted in considerable electron localization and, at least, incipient Fe^{3+} ions in $\text{Fe}_{3-x}\text{Cr}_x\text{O}_4$. The fact that these expectations are not realized argues against localized hopping and are consistent with the effects of impurities on band conduction at low concentration levels. Very similar results have also been observed in $\text{Fe}_{3-x}\text{Al}_x\text{O}_4$, with the area ratio A_β/A_α showing no tendency for the Fe^{2+} and Fe^{3+} B -site occupations to be equal.¹⁰

B. Isomer shifts

As shown in Table IV and Fig. 3, the isomer shift difference between the B -site Fe ions with no Cr^{3+} neighbors and A -site ferric ions is constant for $x < 0.3$ and for $x > 0.3$ decreases as x approaches 0.5. Mössbauer hyperfine parameters at B -site Fe ions with no Cr^{3+} ions at nearest-neighbor B sites are particularly significant because the local configuration giving rise to them is essentially the same as that of pure magnetite except for the conduction-electron concentration. Assuming that the conduction electrons interact more or less equally with all of the B -site ions as in the case of a band description of the itinerant electrons, the constant isomer shift for $x < 0.3$ is consistent with the cation distribution deduced in Sec. IV A in which no ferrous ions are displaced to A sites due to Cr^{3+} substitution.

From this cation distribution $(\text{Fe}^{3+})(\text{Fe}^{2+}\text{Fe}_{1-x}\text{Cr}_x^{3+})\text{O}_4$ the conduction-electron concentration is 0.5 per B site for all x values. The tendency for the isomer shift to become more ferriclike near $x = 0.5$ implies that some of the ferrous ions occupy A sites, thus reducing the number of conduction-electrons per B site. On the other hand, a pair-localized hopping model¹¹ requires that the isomer shift for the $n \neq 0$ B site be constant and independent of x , which is in disagreement with the experimental data of this study.

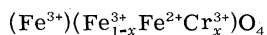
C. Electric quadrupole interactions

The quadrupole splittings at the A and B sites are constant and independent of Cr concentration as shown in Table IV, implying that local symmetries at both A and B are not changed appreciably by Cr^{3+} substitution. This is not surprising since the ionic radius of 0.64 Å for Fe^{3+} is nearly the same as the 0.63 Å ionic radius of Cr^{3+} .

D. Magnetic structure

A canted spin structure was proposed¹ for $\text{Fe}_{3-x}\text{Cr}_x\text{O}_4$ for $x < 0.5$ because the moments deduced

on the basis of a localized, pairwise hopping model and a collinear spin structure would have been in poor agreement with the experimental moments. The calculated moments at 0°K for a pairwise hopping collinear spins for $x=0.25$ and 0.5 are 3.75 and $3.5\mu_B$, respectively, whereas the experimental values are $3.6\mu_B$ for $x=0.25$ and $3.1\mu_B$ for $x=0.5$.¹ It is interesting to note that the cation distribution resulting from this study does not require a canting of the Cr^{3+} spins to explain the magnetic moment data, because the site distribution



gives 3.5 and $3.1\mu_B$ for the values of magnetic moments for $x=0.25$ and 0.5 , respectively. Therefore, it is very likely that Cr^{3+} spins as well as all iron spins are collinear for $x<0.3$, though at higher x values there is without a doubt some canting.

V. CONCLUSION

Through systematic analysis of the Mössbauer spectra of $\text{Fe}_{3-x}\text{O}_4\text{Cr}_x$ ($x=0, 0.05, \frac{1}{8}, \frac{1}{4}, \frac{3}{8}, \frac{1}{2}$) a band description of the conduction electrons and the following cation distribution systematics have been established: when Cr^{3+} ions replace Fe^{3+} ions at B sites of magnetite, no Fe^{2+} ions are displaced from B sites to A sites up to $x=0.3$; for $x>0.3$ small but increasing numbers of Fe^{2+} ions move to A sites as x approaches 0.5 . In support of the above general conclusions, the following specific results have been obtained:

(i) The ratio of the total area of the B subspectrum to that of A subspectrum decreases except for x near 0.5 as required if no Fe^{2+} ions occupy A sites. For x near 0.5 Fe^{2+} ions apparently occupy the A sites but their Mössbauer parameters are similar to those of the B -site Fe ions.

(ii) The isomer shift at the B -site Fe ions that

have no Cr^{3+} neighbors is constant for $x<0.3$ and exhibits a shift toward a more ferric-like charge state as x increases toward 0.5 . Since conduction electrons are delocalized among all B site ions in a band model, these results are consistent with those expected on the basis of the cation distributions: $(\text{Fe}^{3+})[\text{Fe}^{2+}\text{Fe}_{1-x}^{3+}\text{Cr}_x]\text{O}_4$ for $x<0.3$ and $(\text{Fe}_{1-y}^{3+}\text{Fe}_y^{2+})[\text{Fe}_{1-y}^{2+}\text{Fe}_{1-x+y}^{3+}\text{Cr}_x]\text{O}_4$ for $x>0.3$. The conduction-electron concentration is constant for $x<0.3$ and decreases near $x=0.5$ when Fe^{2+} occupies the A site and the number of conduction electrons per B site decreases below 0.5 .

(iii) The magnetic hyperfine field value at B sites with no Cr^{3+} neighbors relative to that at A sites is constant for $x<0.3$ and increases near $x=0.5$. Since a decrease in conduction-electron concentration tends to increase the B site magnetic hyperfine field, these results reflect correctly the effects due to a change in conduction-electron concentration based on the cation distribution systematics of this investigation.

(iv) The cation distribution for low Cr concentration is also found to be in agreement with the magnetic moment data without assuming a canting of the Cr^{3+} spins which is unlikely for low x values.

Finally, the anomalously low value of A_B/A_A reported in Ref. 2 for $x=0.25$ is incorrect and the ^{57}Fe Mössbauer parameters of Fe_3O_4 and their compositional dependence in $\text{Fe}_{3-x}\text{Cr}_x\text{O}_4$ provide incontrovertible evidence of the validity of a band model for the electronic conduction mechanism in Fe_3O_4 , in agreement with recent theoretical predictions.¹²

ACKNOWLEDGMENT

The support of this investigation by the National Science Foundation is gratefully acknowledged.

*On leave from Department of Physics, Yonsei University, Seoul, Korea.

¹M. Robbins, G. K. Wertheim, R. C. Sherwood, and D. N. E. Buchanan, *J. Phys. Chem. Solids* **32**, 717 (1971).

²A. S. Bukin, A. K. Gapeev, R. N. Kuzmin, and A. A. Novakova, *Kristallogr.* **17**, 799 (1972) [*Sov. Phys.-Crystallogr.* **17**, 701 (1973)].

³L. Néel, *Ann. Phys.* **3**, 137 (1948).

⁴M. A. Butler, M. Eibschütz, and L. G. Van Uitert, *Solid State Commun.* **12**, 499 (1973).

⁵K. Motida and S. Miyahara, *J. Phys. Soc. Jpn.* **28**, 1188 (1970).

⁶R. W. Wyckoff, *Crystal Structures* (Interscience, New York, 1965), Vol. 3, p. 79.

⁷S. L. Ruby, B. J. Evans, and S. S. Hafner, *Solid State Commun.* **6**, 277 (1968); W. E. Sauer and R. J. Reynik, in *Mössbauer Effect Methodology*, edited by

I. J. Gruverman (Plenum, New York, 1968), Vol. IV, p. 201; G. K. Wertheim, V. Jaccarino, J. H. Wernick, and D. N. E. Buchanan, *Phys. Rev. Lett.* **12**, 24 (1964); M. B. Stearns, *Phys. Rev.* **147**, 439 (1966).

⁸B. J. Evans, in *Mössbauer Effect Methodology*, edited by I. J. Gruverman (Plenum, New York, 1968), Vol. IV, p. 139.

⁹G. A. Sawatzky, F. van der Woude, and A. H. Morrish, *Phys. Rev.* **183**, 383 (1969).

¹⁰G. Dehe, B. Seidel, C. Michalk, and K. Melzer, in *Proceedings of the Fifth International Conference on Mössbauer Spectroscopy*, edited by M. Hucl and T. Zemtík (Czechoslovak Atomic Energy Commission, Prague, 1975), Part 1, p. 106.

¹¹J. M. Daniels and A. Rosenzweig, *J. Phys. Chem. Solids* **30**, 1561 (1969).

¹²B. Lorenz and D. Ihle, *Phys. Status Solidi B* **69**, 451 (1975).